World Academy of Science, Engineering and Technology
International Journal of Aerospace and Mechanical Engineering
Vol:3, No:10, 2009

Design and Characteristics of New Test Facility for Flat Plate Boundary Layer Research

N. Patten, T. M. Young, and P. Griffin

Open Science Index, Aerospace and Mechanical Engineering Vol:3, No:10, 2009 publications.waset.org/9275/pdf

***Abstract*—**Preliminary results for a new flat plate test facility are presented here in the form of Computational Fluid Dynamics (CFD), flow visualisation, pressure measurements and thermal anemometry. The results from the CFD and flow visualisation show the effectiveness of the plate design, with the trailing edge flap anchoring the stagnation point on the working surface and reducing the extent of the leading edge separation. The flow visualization technique demonstrates the two-dimensionality of the flow in the location where the thermal anemometry measurements are obtained. Measurements of the boundary layer mean velocity profiles compare favourably with the Blasius solution, thereby allowing for comparison of future measurements with the wealth of data available on zero pressure gradient Blasius flows. Results for the skin friction, boundary layer thickness, frictional velocity and wall shear stress are shown to agree well with the Blasius theory, with a maximum experimental deviation from theory of 5%. Two turbulence generating grids have been designed and characterized and it is shown that the turbulence decay downstream of both grids agrees with established correlations. It is also demonstrated that there is little dependence of turbulence on the freestream velocity.

***Keywords*—**CFD, Flow Visualisation, Thermal Anemometry, Turbulence Grids.

I. Introduction

THE ability to predict transition is becoming an ever more important requirement in many areas of engineering and plays an essential role in many aerodynamic applications where the desire to employ large regions of laminar flow is advantageous. The development of theoretical methods for transition prediction depends on sufficiently detailed experimental data to describe the complex physical processes involved. The effect of freestream turbulence (FST) on the onset of transition has received great attention in the last number of years [1]-[5], and is of great interest, for example, in the area of turbine blade design, where the impingement of turbulence from the wake of the stator influences the boundary layers on the rotor blades [6]. It is widely known that an elevated FST level causes transition to occur more rapidly. Reference [7] introduced the term 'bypass' transition and this type of transition can occur in the presence of large, nonlinear disturbances (e.g. elevated FST, usually above 1% of the freestream velocity). Amplitude and spectral characteristics of the disturbance strongly influence which type of transition occurs. Transient growth occurs when two nonorthogonal, stable modes interact and grow [8]. The path to transition for the lowest freestream disturbance levels does not include transient growth. However, as the FST amplitude is increased, a point is reached where the primary modes are bypassed completely. At elevated FST levels, if the disturbance amplitudes are large enough, the boundary layer undergoes transition below the critical Reynolds number predicted by linear stability theory. An understanding of the physical mechanisms by which FST affects boundary layer transition is essential for transition prediction and control. Predicting the location of transition in the boundary layer is very important for the advanced design of aerodynamic vehicles as the skin friction and heat transfer in the laminar and turbulent regime are different [9]. The Reynolds number, the FST, surface roughness, surface temperature and the pressure gradient are some of the known parameters effecting the location of laminar to turbulent transition [10]-[11].

From an experimental perspective, there are essential factors that determine the receptivity of the boundary layer to FST. The geometry of the leading edge plays a key role in minimising leading edge separation and pressure gradients along the working surface [2], [3], [10]. The nature of the disturbance is also important; bypass transition occurring if the amplitude of the forced disturbances is large [12]. To understand the fundamental mechanisms involved, it is necessary to obtain detailed spectral characteristics of the flow phenomena present in the boundary layer.

The easiest test surface for investigating the effects of various parameters to the underlying boundary layer is the 'universal' flat plate. Although the boundary layer occupies geometrically only a small portion of the flow field, its influence on drag and heat transfer to the body is immense [13]. The boundary layer that develops on the surface of a body usually starts as a laminar layer, but in most situations, inevitably becomes turbulent. The key in any flow control technique is the realisation that transition is an eventual stage in a process involving the amplification of disturbances. Either the amplification or the disturbance itself must be eliminated in order to favour laminar flow. A known effect of turbulence is to improve the mixing in the flow [14]. This means that distant parts of the flow are brought closer together, even if they have very different properties, due to the turbulent motion of the flow. A turbulent boundary layer is therefore more uniform compared to a laminar one because the momentum diffusion in the laminar flow is much slower. In

N. Patten is with the Mechanical and Aeronautical Engineering Department, University of Limerick, Ireland (353-61-213134; e-mail: norah.patten@ul.ie).

T. M. Young is with the Mechanical and Aeronautical Engineering Department, University of Limerick, Ireland.

P. Griffin is with the Mechanical and Aeronautical Engineering Department, University of Limerick, Ireland.

the analysis of transitional flows, discrimination between laminar and turbulent flows is valuable not only to estimate the intermittency function but also to obtain separate statistics of the measured data for laminar and turbulent cases. The intermittency is the fraction of time the flow is turbulent [15]. The objectives of the current study are to design, manufacture and characterise a new flat plate for zero pressure gradient boundary layer research. In addition, it is necessary to characterise the turbulence generating grids and compare results to established correlations.

II. Flat plate Design, Experimental facility and measurement techniques

A. Flat plate design

When performing a study on zero pressure gradient flows, a critical part of the experiment that must be addressed is the leading edge of the plate. It is essential to avoid flow separation and instability since this would corrupt downstream measurements. The flat plate used for this study is similar in design to the plate used by Hernon et al. (2007) [16]. To ensure maximum effectiveness of the design, there are a number of crucial design steps that must be adhered to. The stagnation line location has a considerable influence on the boundary layer development. An adjustable trailing edge flap ensures the stagnation point is fixed on the upper test surface, therefore the boundary layer develops smoothly and a negligible streamwise pressure gradient is achievable [3], [10], [16], [17]. A small gap between the test section walls and the plate edges was employed to hinder propagation of disturbances and the plate employs a small leading edge radius [16], [17]. With these key factors noted, the flat plate design comprises of a leading edge radius of 2mm with a 5 degree chamfer to the lower surface and a trailing edge adjustable flap, designed for both positive and negative angles (Fig. 1). The plate is manufactured in three sections to allow for a range of experimental configurations, is made from 10mm thick aluminium and is approximately 1m long by 0.290m wide. Preliminary investigation of the design was obtained through Computational Fluid Dynamics (CFD) analysis, followed by flow visualisation using a mixture of powder particles and paraffin oil, surface pressure measurements and hotwire anemometry. There are 15 surface pressure measurement stations along the plate in the flow direction. The static pressure was measured through 0.5mm diameter holes on the surface, which were connected to a manometer and allowed for the calculation of the static pressure along the working surface of the plate.

All measurements were obtained in a non-return type wind tunnel with continuous airflow supplied by a centrifugal fan, powered by a 70kW electric motor. The test section is 0.3 x 0.3m^2 by 1m long. Maximum velocities in excess of 100m/s can be achieved.

TABLE I
Units for Properties

Symbol	Quantity	SI units
d	Diameter	m
P	Pressure	N/m^2
P_∞	Freestream Pressure	N/m^2
u	Local velocity	m/s
U_∞	Freestream velocity	m/s
U_e	Boundary layer edge velocity	m/s
x	Streamwise distance	m
y	Wall normal distance	m
Tu	Turbulence intensity	–
RMS	Root mean square	–
u^+	Non-dimensional streamwise velocity	–
y^+	Non-dimensional wall normal distance	–
Re_x	Reynolds number based on streamwise distance	–
Re_θ	Reynolds number based on momentum thickness	–
ρ	Density	Kg/m^3
δ	Boundary layer thickness	M
u_τ	Frictional velocity	m/s
C_f	Skin friction coefficient	–
η	Blasius parameter	–
μ	Dynamic viscosity	Ns/m^2

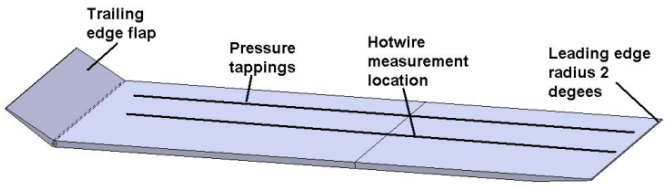


Fig. 1: Flat plate design features and measurement locations

B. CFD Analysis

The effectiveness of the plate design was investigated by means of CFD using the software package Fluent 6.3, with the 2D, steady laminar flow solver. The model was meshed using Gambit 2.2 and consisted of 130,000 cells. A grid sensitivity test was undertaken by reducing the mesh size to 50,000 cells and the solution was found to be grid independent. The CFD analysis is used to gain information about the preliminary design of the flat plate. Key features of the flat plate include the leading edge and the trailing edge flap. CFD was used as a preliminary design tool to validate the effectiveness of these features.

The effectiveness of the trailing edge flap in anchoring the stagnation point on the upper surface is shown in Fig. 2. With the trailing edge flap in operation at 40°, the extent of the separation at the leading edge of the plate is reduced. This allows control of the pressure distribution in this region and along the working surface. The velocity vectors (Fig. 2(a)) clearly show that for a flap angle of 40° the stagnation point moves from the leading edge to the upper surface. The velocity contours (Fig. 2(b)) show the stagnation point at the leading edge of the plate for a flap angle of 0°.

Open Science Index, Aerospace and Mechanical Engineering Vol:3, No:10, 2009 publications.waset.org/9275/pdf

Open Science Index, Aerospace and Mechanical Engineering Vol:3, No:10, 2009 publications.waset.org/9275/pdf

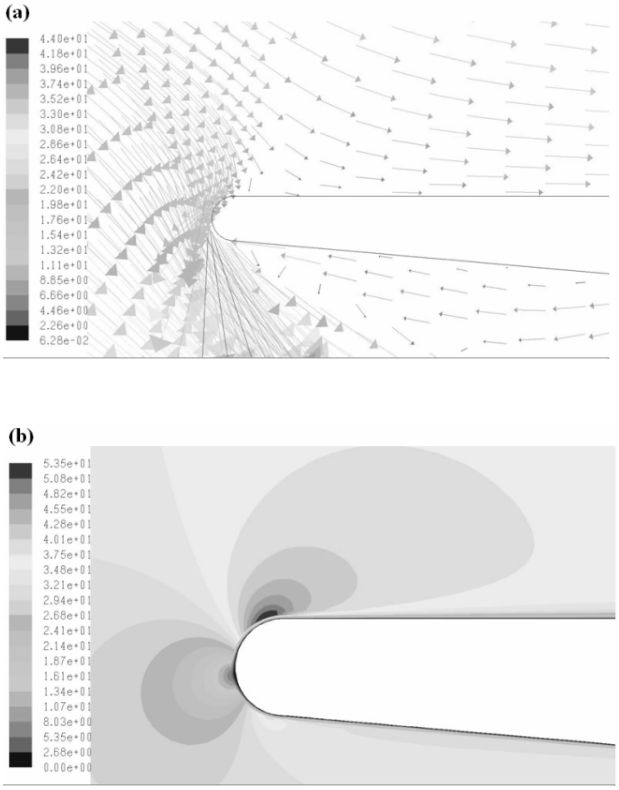


Fig. 2: (a) Velocity vectors coloured by velocity magnitude; trailing edge flap 40°. (b) Velocity contours coloured by velocity magnitude; trailing edge flap angle 0°

It is also demonstrated using CFD that the boundary layer along the flat plate at zero incidence favourably follows the Blasius profile (Fig. 3). The formation of the boundary layer is greatly influenced by the shape of the leading edge of the plate as well as any pressure gradient that may exist in the flow. These preliminary measurements are essential in order to optimise the flat plate and address some of the critical aspects related to its design.

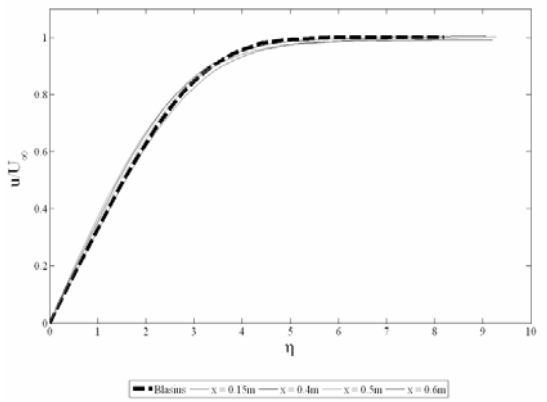


Fig. 3: CFD comparison to Blasius profile at various locations along the plate with trailing edge flap angle of 40°.

C. Flow Visualisation

Much information on flow behaviour has been obtained from simple techniques to make localised movements visible [18]. Flow visualisation using a mixture of powder particles and paraffin oil was utilised to observe flow phenomena over the length of the plate, ensuring no adverse flow occurred. The surface of the plate was spray painted black to a matt finish, ensuring a good contrast between the plate surface and the powder particles. Fig. 4 and Fig. 5 illustrate the flow pattern over the length of the plate with the flap angle set to 0° and 40° respectively. It is evident that with the flap at 40°, the leading edge separation is reduced significantly, from approximately 10mm to 3mm.



Fig. 4: Flow visualization over the plate with trailing edge flap at 0°. Entire plate and close up of leading edge.

The two dimensionality of the flow field is also evident in Fig. 4. In Fig. 5 the three dimensionality of the flow field is evident close to the edges of the plate, however, this is not in the region of measurement location.

D. Experimental Setup and Measurement Techniques

All measurements were obtained in a non-return type wind tunnel with continuous airflow supplied by a centrifugal fan powered by a 70kW electric motor. The boundary layer traverses were obtained using a single normal Dantec hotwire probe (55P11) operated in the constant temperature (CTA) mode with an overheat temperature of 250°C. Measurements were recorded over 13 seconds at a sampling frequency of 20kHz and were low pass filtered at 10kHz to remove any noise at higher frequencies and prevent aliasing. The traverse mechanism allows for incremental movements of the hotwire of 10μm, sufficient for near wall measurement accuracy. During any boundary layer traverse, the temperature in the test section was maintained constant to within 0.1°C. The background turbulence intensity in the test section was measured to be 0.2%.

Open Science Index, Aerospace and Mechanical Engineering Vol:3, No:10, 2009 publications.waset.org/9275/pdf



Fig. 5: Flow visualization over the plate with trailing edge flap at 40°. Entire plate and close up of leading edge.

The plate is positioned in the centre of the tunnel and is supported by means of two aluminium brackets on the lower surface. The heat loss from a hotwire can be employed to measure the local velocity in the flow field if the convective heat loss is known as a function of the effective cooling velocity. This is usually obtained through the calibration of the hotwire anemometer output in a known velocity field. If the test surface wall consists of a heat conducting material (e.g. metal) as the hotwire approached the wall, the anemometer output increases beyond the values corresponding to the local velocity at the wall distance where the wire is located [20]. In the current investigation, the near wall measurements affects by wall conduction have been deleted prior to post processing of the data.

III. Results

A. Comparison of results to the Blasius profile

It is well known that all velocity profiles tend toward zero at the wall and that τ_w, the shearing stress at the wall, is constant where the velocity profile matches the linear law of the wall [16], [20], [21]. Fig. 6(a) shows an example of the velocity profile in wall units compared to the linear law of the wall. Since the velocity profile compares favourably to the linear law of the wall ($u^+ = y^+$) the near wall resolution is sufficient to allow for accurate calculation of τ_w. The wall location (y = 0) position was found by linearly extrapolating the velocity versus position data to the wall (Fig. 6(b)).

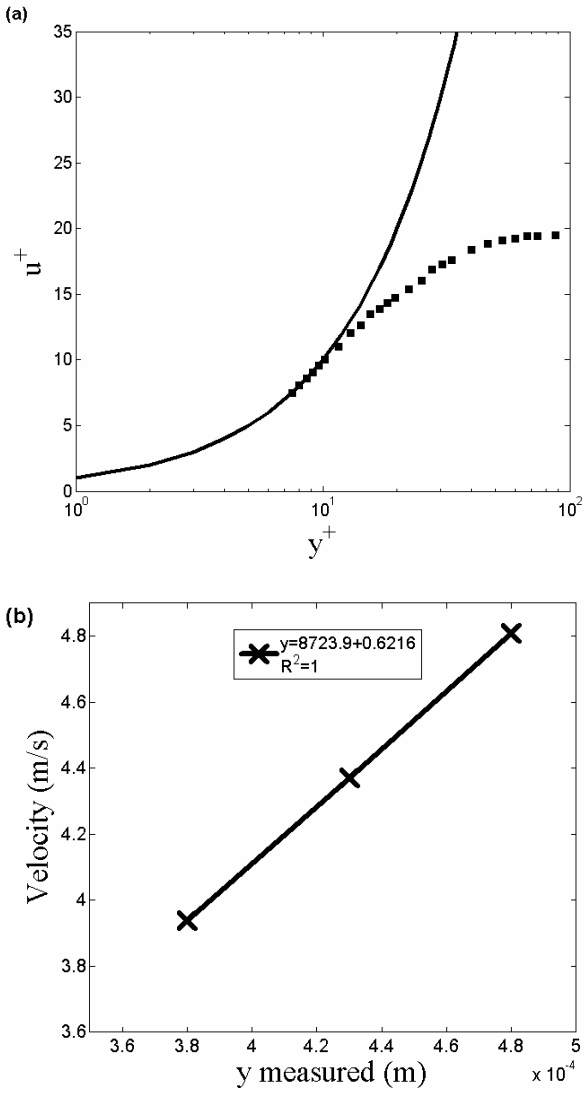


Fig. 6: (a) Velocity profile compared to linear law of the wall. (— linear law of the wall; • measured velocity profile) (b) Linear region of measured velocity profile, extrapolated to find the wall position

It is essential that the flat plate agrees favourably to the zero pressure gradient Blasius profile in order to compare future measurements with that of the wealth of experiments in the literature. Fig. 7(a) shows a comparison of the experimental data to that of theory and it is shown that excellent agreement was possible. The pressure distribution along the plate was measured using a Furness Control Limited FC012 Digital manometer, with 15 pressure taps along the working surface. The velocity distribution (Fig. 7 (b)) along the length of the plate remains constant, except in the most upstream region, which was measured 25mm downstream of the leading edge. The pressure readings from the manometer were converted into velocities using the following equation:

Open Science Index, Aerospace and Mechanical Engineering Vol:3, No:10, 2009 publications.waset.org/9275/pdf

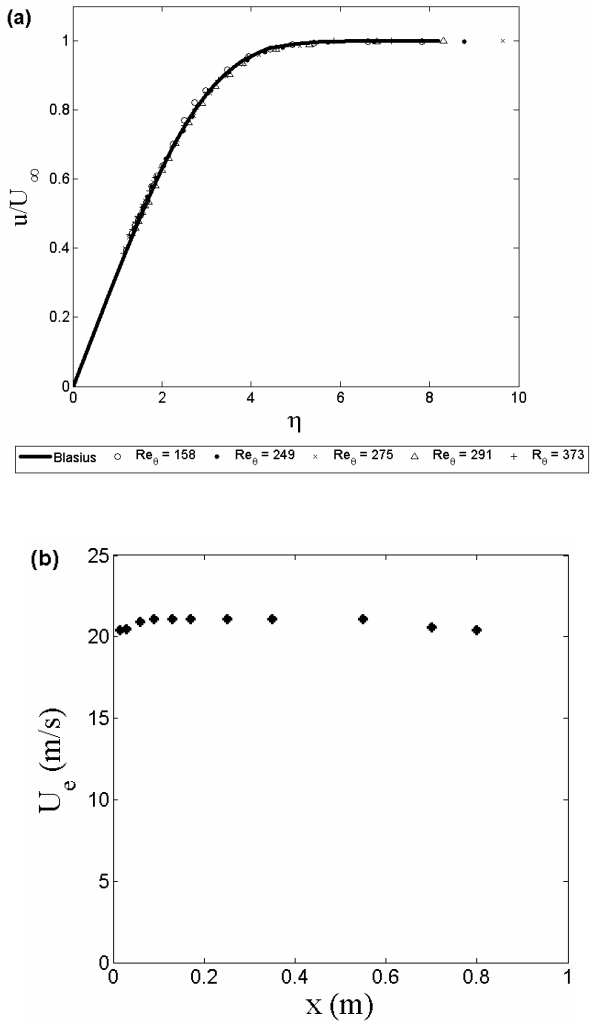


Fig. 7: (a) Mean velocity profiles over the plate compared to the Blasius profile. (b) Velocity distribution over the plate using (1).

$$P - P_{\infty} = \frac{1}{2}\rho U_{\infty}^{2}\left(1 - \frac{U}{U_{\infty}}\right)^{2} \quad (1)$$

The theoretical boundary layer thickness is obtained using (2).

$$\delta = 5\sqrt{\frac{\nu x}{U_{\infty}}} \quad (2)$$

The experimental boundary layer thickness is describes as the location from the wall where the velocity is 99% of the freestream velocity.

The theoretical and experimental wall shear stresses are calculated using (3) and (4) respectively.

$$\tau_w = \frac{0.664\,\rho U_{\infty}^{2}}{2\sqrt{\mathrm{Re}_x}} \quad (3)$$

$$\tau_w = \mu\left(\frac{du}{dy}\right)_{y=0} \quad (4)$$

The theoretical and experimental frictional velocities are calculated using (5) and (6) respectively.

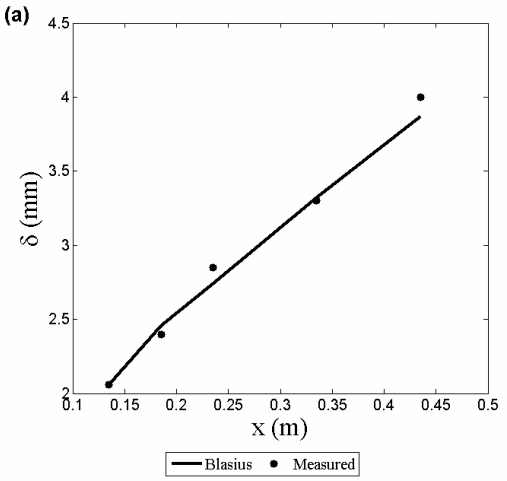
$$u_{\tau} = \frac{0.576 U_{\infty}}{(\mathrm{Re}_x)^{0.25}} \quad (5)$$

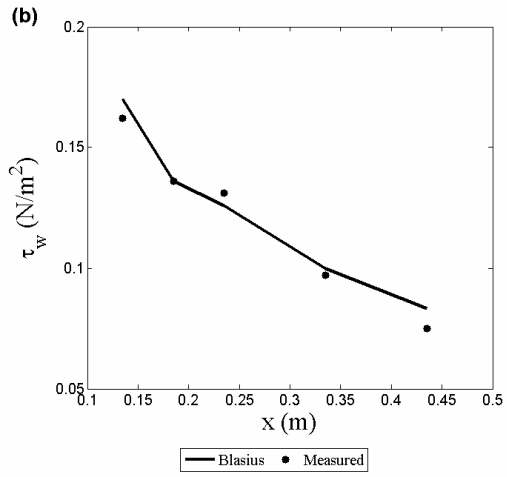
$$u_{\tau} = \sqrt{\frac{\tau_w}{1.2}} \quad (6)$$

The theoretical and experimental skin friction coefficients are calculated using (7) and (8) respectively.

$$c_{f_x} = \frac{0.664}{\sqrt{\mathrm{Re}_x}} \quad (7)$$

$$c_{f_x} = \frac{2\tau_w}{\rho_{\infty} U_{\infty}} \quad (8)$$





Open Science Index, Aerospace and Mechanical Engineering Vol:3, No:10, 2009 publications.waset.org/9275/pdf

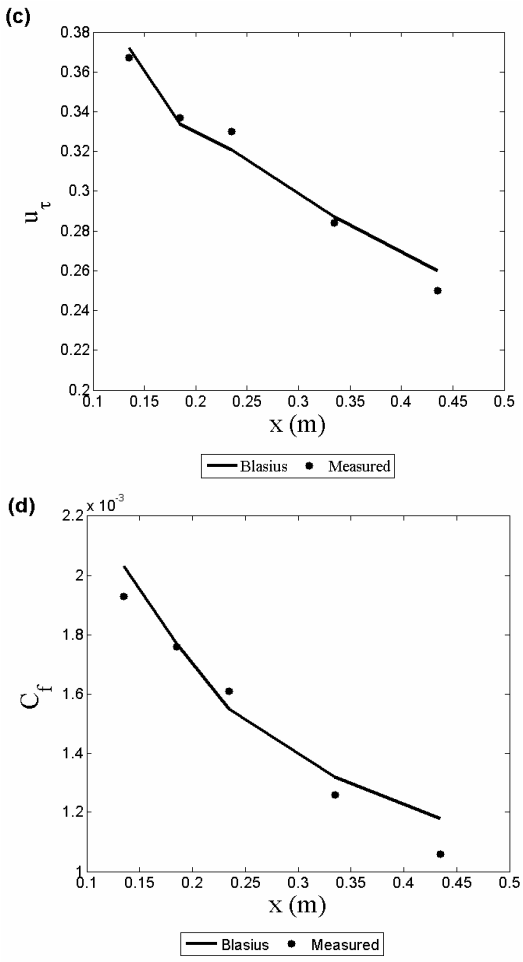


Fig. 8: Comparison of theoretical Blasius to experimental results. (a) Boundary layer thickness. (b) Wall shear stress. (c) Frictional velocity. (d) Skin friction coefficient

Fig. 8 (a), (b), (c) and (d) demonstrate the excellent agreement between the theoretical Blasius solutions compared to the measured experimental results, giving confidence in the measurement technique and the data acquisition and reduction.

B. Turbulence grid design and characterization

The simplest and most convenient method of generating turbulence is by means of grids. In order to provide the necessary FST levels, two grids have been designed and characterized. The first grid was designed to produce large FST levels and is a perforated plate (PP) made from a 5mm thick aluminum plate. The second grid was designed to produce much lower FST levels and is a square mesh of round bars (SMR).

Equations (2) and (3) give the power–law relation of [22] for the turbulence decay downstream of the PP and SMR respectively.

$$Tu = 1.13(x/d)^{-5/7} \quad (2)$$

$$Tu = 0.8(x/d)^{-5/7} \quad (3)$$

Fig. 9 (a) demonstrates that excellent agreement with the power–law relation of [22] was possible with both grids. Fig. 9(b) shows there is little dependence of the FST on velocity change.

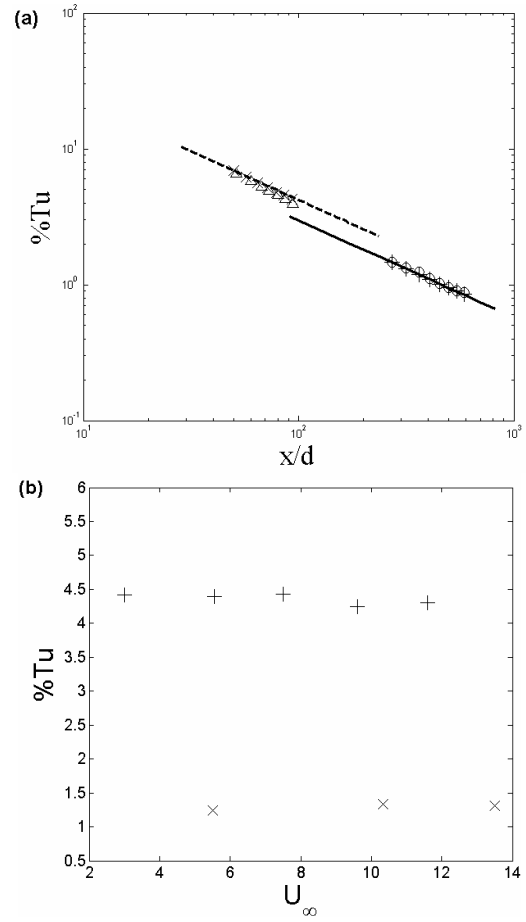


Fig. 9: (a) Turbulence decay downstream of each grid compared to the Roach (1987) correlation. (— = $1.13(x/d)^{-5/7}$; --- = $0.8(x/d)^{-5/7}$; + = SMR, Re_d = 1000; o = SMR, Re_d = 750; Δ = PP, Re_d = 2500; x = PP, Re_d = 1400. Re_d is the Reynolds number based on the thickness of the grid bar/wire). (b) Turbulence intensity dependence on freestream velocity. (+ = large grid at 0.4m from grid; x = small grid at 0.35m from grid).

IV. Conclusion

- Preliminary investigations through CFD verified the effectiveness of a new flat plate design, with the trailing edge flap anchoring the stagnation point in the upper surface.
- Using flow visualization, the two dimensionality of the flow field was confirmed and the trailing edge flap was shown to reduce leading edge separation from 10mm to 3mm when positioned at 40°.
- Through thermal anemometry, it was shown that measurements along the flat plate compare favourably to the Blasius profile.
- Sufficient near wall resolution was confirmed due to the velocity profiles matching the linear law of the wall.
- Comparison between the experimentally measured boundary layer thickness, skin friction, frictional

velocity and wall shear stress and were found to deviate no more than 5% from the Blasius solutions.

- The characteristics of two turbulence generating grids show excellent agreement with the power–law relation of Roach (1987) and that there was little dependence of turbulence on freestream velocity.

REFERENCES

[1] M. F. Blair, "Boundary Layer Transition in Accelerating Flows with Intense Freestream Turbulence: Part 1 - Disturbances Upstream of Transition Onset", *J. Turbomachinary*, Vol. 114, 1992, pp. 313 - 321.

[2] J. Fransson, M. Matsubara, and P. Alfredsson, "Transition Induced by Freestream Turbulence", *J. Fluid Mechanics*, Vol. 527, 2005, pp. 1–25.

[3] P. E. Roach, and D. H. Brierley, "The Influence of a Turbulent Free-Stream on Zero Pressure Gradient Transitional Boundary Layer Development", Part 1 test cases t3a and t3b: ERCOFTAC Workshop, Lausanne, France, 1990.

[4] M. Matsubara, and P. Alfredsson, "Disturbance Growth in Boundary Layers Subjected to Freestream Turbulence", *J. Fluid Mechanics*, Vol. 430, 2001, pp. 149–168.

[5] J. Wesin, "Laminar – Turbulent Boundary Layer Transition Influenced by Freestream Turbulence". PhD dissertation, Dept. Mechanics, KTH, Stockholm, Sweden, 1997.

[6] K. J. Westin, A. V. Boiko, B. G. Klingmann, V. V. Kozlov, and P. H. Alfredsson, "Experiments in a Boundary Layer Subjected to Free Stream Turbulence. Part 1. Boundary Layer Structure and Receptivity", *J. Fluid Mechanics*, Vol. 281, 1994, pp. 193-218.

[7] M. V. Morkovin, "Bypass Transition to Turbulence and Research Desiderata", *Transition in Turbines*, NASA-CP-2386, 1984, pp.161-294.

[8] W. Saric, H. Reed, and E. Kerschen, "Boundary-Layer Receptivity to Freestream Disturbances", *Annual Rev. Fluid Mechanics*, Vol. 34, 2002, pp. 291–319.

[9] T. Herbert, "Boundary Layer Transition – Analysis and Prediction Revisited", AIAA-91-0737, 29th Aerospace Sciences Meeting. Jan 7-10, Reno, Nevada, 1991.

[10] V. M. Filippov, "Influence of Plate Nose Heating on Boundary Layer Development", *J. Fluid Dynamics* , Vol. 37, No. 1, 2002, pp. 27-36.

[11] B. Abu-Ghannam, and R. Shaw, "Natural Transition of Boundary Layers - The Effects of Turbulence, Pressure Gradient, and Flow History", IMechE 22, 1980, pp 213–228.

[12] K. H. Sohn, J. E. O'Brien, and E. Reshotko, "Some Characteristics of Bypass Transition in a Heated Boundary Layer", NASA TM 102126, 1989.

[13] J. P. Holman, *Heat Transfer*, 8th Edition, New-York; London: McGraw-Hill, USA, 1997.

[14] J. Cousteix, "Basic Concept on Boundary Layers", AGARD Report No. 786, Special Course on Skin Friction Drag Reduction, 1992.

[15] D. Zhou, and T. Wang, "Effects of Elevated Freestream Turbulence on Flow and Thermal Structures in Transitional Boundary Layers", *J. Turbomach*, Vol. 117, 1995, pp. 407 – 417.

[16] D. Hernon, E. J. Walsh, and D. M. McEligot, "Experimental Investigation into the Routes to Bypass Transition and Shear-Sheltering Phenomenon". *J. Fluid Mechanics*, Vol. 591, 2007, pp. 461-479.

[17] S. Becker, C. M. Stoots, K. G. Condie, F. Dursk, and D. M. McEligot, "LDA-Measurements of Transitional Flows Induced by a Square Rib", *J. of* Fluid Engineering, Vol. 124, Issue 1, 2002, pp. 108 – 118.

[18] W. Merzkirch, *Flow Visualisation II*, New York: Academic Press, 1982.

[19] H. Schlichting, *Boundary Layer Theory*. 7th edition, McGraw-Hill, USA, 1979.

[20] J. C. Bhatia, F. Durst, and J. Jovanovic, "Correction of Hotwire Anemometry Measurements Near Walls". *J. Fluid Mechanics*, Vol. 122, 1982, pp. 411–431.

[21] J. Kim, and T. W. Simon, "Freestream Turbulence and Concave Effects on Heated, Transitional Boundary Layers". NASA CR 187150, Vol. 1, 1991.

[22] P. E. Roach, "The Generation of Nearly Isotropic Turbulence by means of Grids", *Heat and Fluid Flow*, Vol. 8, No. 2, 1987.

Open Science Index, Aerospace and Mechanical Engineering Vol:3, No:10, 2009 publications.waset.org/9275/pdf